The deep Earth may not be cooling down

The deep Earth may not be cooling down

Denis Andrault[1,*], Julien Monteux[1], Michael Le Bars[2] and Henri Samuel[3]

[1] Laboratoire Magmas et Volcans, CNRS-OPGC-IRD, Université Blaise Pascal, Clermont-Ferrand, France

[2] CNRS, Aix-Marseille Université, Ecole Centrale Marseille, IRPHE, UMR 7342, Marseille, France

[3] Institut de Recherche en Astrophysique et Planétologie, CNRS, Université Paul Sabatier, Toulouse, France

Abstract

The Earth is a thermal engine generating the fundamental processes of geomagnetic field, plate tectonics and volcanism. Large amounts of heat are permanently lost at the surface yielding the classic view of the deep Earth continuously cooling down. Contrary to this conventional depiction, we propose that the temperature profile in the deep Earth has remained almost constant for the last ~4.3 billion years. The core-mantle boundary (CMB) has reached a temperature of ~4400 K in probably less than 1 million year after the Moon-forming impact, regardless the initial core temperature. This temperature corresponds to an abrupt increase in mantle viscosity atop the CMB, when ~60% of partial crystallization is achieved, accompanied with a major decrease in heat flow at the CMB. Then, the deep Earth underwent a very slow cooling until it reached ~4100 K today. This temperature at, or just below, the mantle solidus is suggested by seismological evidence of ultra-low velocity zones in the D"-layer. Such a ~steady thermal state of the CMB temperature excludes thermal buoyancy from being the predominant mechanism to power the geodynamo over geological time.

An alternative mechanism to sustain the geodynamo is mechanical forcing by tidal distortion and planetary precession. Motions in the outer core are generated by the conversion of gravitational and rotational energies of the Earth-Moon-Sun system. Mechanical forcing remains efficient to drive the geodynamo even for a sub-adiabatic temperature gradient in the outer core. Our thermal model of the deep Earth is compatible with an average CMB heat flow of 3.0 to 4.7 TW. Furthermore, the regime of core instabilities and/or secular changes in the astronomical forces could have supplied the lowermost mantle with a heat source of variable intensity through geological time. Episodic release of large amounts of heat could have remelted the lowermost mantle, thereby inducing the dramatic volcanic events that occurred during the Earth's history. In this scenario, because the Moon is a necessary ingredient to sustain the magnetic field, the habitability on Earth appears to require the existence of a large-satellite.

* Corresponding author: denis.andrault@univ-bpclermont.fr

Key Words: Temperature profile in the deep Earth, Secular cooling of the Earth, Generation of the geomagnetic field.

Highlights:

- We review the early and the present thermal states of the deep Earth
- We highlight the paradoxes implied by the classical scenario based on secular cooling
- We propose a 4.3 Gy steady thermal state scenario for the lowermost mantle
- We suggest the Moon as a necessary ingredient to sustain the Earth's magnetic field

Acknowledgements: We thank D. Cébron, B. Favier, R. Ferrari, H. Martin and the anonymous reviewers for fruitful discussions and help. This work has gained value from previous collaborative works with N. Bolfan-Casanova, M.A. Bouhifd, M. Mezouar and G. Morard. This is an ANR-OxyDeep and ANR-Clervolc contribution n°XX.

1. Introduction

Our knowledge of the present-day thermal state of the deep Earth has largely improved based on comparisons between seismic observations and experimental and theoretical characterisations of the Earth's materials, including studies of phase transitions and melting curves. In addition, we now have a more precise idea of the early evolution of the deep Earth based on paleomagnetic and geochemistry data as well as numerical modelling. However, the path the deep Earth has followed from its early formation to its current state remains puzzling. In particular, the Earth's heat budget over the ~4.5 billion years (Gy) of its existence remains difficult to balance satisfactorily. In this article, we challenge the classical view that the Earth is continuously cooling. We propose an alternative model for the thermal and magnetic evolution of the deep Earth. First, we review the early and the present thermal states of the deep Earth (sections 2 and 3), then we highlight the major paradoxes implied by the classical scenario based on secular cooling (section 4). Finally, we propose a steady thermal state scenario (section 5) involving an alternative source of energy to power the geodynamo: precession and tides (sections 6 and 7). The implications of this scenario are presented in the final section.

2. The early temperature profile in the deep Earth

2.1 The primordial core

The initial core temperature is related to a variety of processes but primarily results from the mechanism of core-mantle segregation (Stevenson, 1990). Metal/silicate separation is a rapid event (<60 My) contemporaneous with the Earth's accretion from many planetary embryos (Kleine et al., 2002; Rudge et al., 2010). After a meteoritic impact, the Fe-droplets produced by fragmentation of the impactor's core descended and equilibrated thermally in a highly turbulent magma ocean (Deguen et al., 2011; Samuel, 2012; Wacheul et al., 2014). The resulting iron layer/pond that formed at the bottom of the magma ocean then descended through the underlying, more viscous mantle in the form of diapirs or, alternatively, through channels (Stevenson, 1990). In both cases, the corresponding gravitational potential energy released was dissipated into heat, but the heat partitioning between the iron and the silicate depends on the segregation mechanism (Rubie et al., 2015). The diapir mechanism tends to favor heat transfer to the viscous mantle (Monteux et al., 2009; Samuel et al., 2010), while channels favor a hotter core (Ke and Solomatov, 2009), yielding a wide range of plausible thermal states at the core-mantle boundary. If metal-silicate thermal equilibration had been efficient, the initial core temperature would be similar to that of the lowermost mantle. Taking into consideration the contributions of heating from large impacts and the decay of short-lived radionuclides, the early core was likely to be hotter than the mantle liquidus soon after its formation (Rubie et al., 2015).

87 *2.2 From the magma ocean to the mantle*

88 The giant Moon forming impact (MFI) that occurred ~60 million years (My) after the Earth's
89 formation (Touboul et al., 2007), likely re-melted the entire mantle (Nakajima and Stevenson, 2015)
90 and significantly heated up the Earth's core (Herzberg et al., 2010) (Fig. 1a). The MFI, through the
91 release of energy induced by gravitational segregation of the impactor's core, could have potentially
92 increased the core temperature further by 3500–4000 K (Rubie et al., 2015). This could have resulted
93 in an initial CMB temperature on the order of 6000 K (Nakagawa and Tackley, 2010), which is well
94 above the mantle solidus of ~4150 K (Andrault et al., 2011; Fiquet et al., 2010). Therefore, the MFI
95 could have caused intensive melting in the lowermost mantle.

96 Upon cooling of this giant-impact induced magma ocean, a thin crust rapidly formed at the
97 surface, within the cold upper thermal boundary layer (Solomatov, 2015) (Fig. 1b). Just below, the
98 magma ocean is expected to have convected vigorously. Hence, its internal temperature would follow
99 an adiabatic profile undergoing a progressive decrease in potential surface temperature with time
100 (Abe, 1997; Solomatov, 2000). Due to the fact that the liquidus and solidus curves present P-T slopes
101 steeper than the magma ocean adiabats for the chondritic-type composition (Andrault et al., 2011;
102 Thomas and Asimow, 2013), the magma ocean should solidify from the bottom up (Fig. 1b). The
103 heat flux at the surface could have been as high as ~10^6 W/m^2, which suggests crystallization of most
104 of the magma ocean within ~10^3 years (Solomatov, 2015). However, the situation may have been
105 complicated by physical and chemical processes such as suspension, turbulence, nucleation, and
106 percolation or by the formation of an opaque atmosphere at the Earth's surface. These effects could
107 delay the complete crystallization of the upper mantle up to 10^8 years after the magma ocean began
108 cooling (e.g. after the MFI) (Fig. 1c and 1d) (Lebrun et al., 2013; Sleep et al., 2014).
109
110 **3. The present-day temperature profile in the deep Earth**

111 *3.1 Upper mantle, transition zone and the lower mantle*

112 The temperature profile from the shallow mantle to a few hundred kilometers above the CMB is
113 relatively well documented. The most robust constraints originate from the phase transformations at
114 the 410, 520 and 660 km discontinuities; the depth of the phase transformations must be compatible
115 with the phase diagram of the major upper mantle minerals, mainly olivine, which is well constrained
116 experimentally. When including the effect of entropy variations between the different polymorphs, a
117 temperature discontinuity of a few hundred degrees is induced at the seismic discontinuities (Katsura
118 et al., 2010; Stacey and Davis, 2008). Complications in the temperature determination using the
119 olivine phase diagram may arise from the uncertainties in mantle concentrations of FeO, water and
120 ferric iron (e.g. (Frost and Dolejs, 2007)), because they modify the pressure of the phase transitions
121 slightly. Lateral temperature variations are also expected from colder temperatures in subduction

zones to hotter temperatures in regions of upwelling mantle (ocean ridges, for example). Altogether, the uncertainty is less than a couple of hundred degrees. Then, the temperature profile in the lower mantle is classically extrapolated from anchor points in the transition zone using an adiabatic gradient, which yields additional uncertainties. Slightly different temperature profiles can be obtained, depending on the equations of states used for the mantle (Brown and Shankland, 1981; Stacey and Davis, 2008). Other predictions give a significantly higher temperature profile when refining the seismic profiles (*Vp*, *Vs*, ρ) from the mineral equations of states (ρ, *K*, *G*) (Matas et al., 2007) (Fig. 2a).

3.2 The lowermost mantle

The thermal state of the lowermost mantle is not directly correlated to the surface potential temperature, but is rather tied to the temperature of the core and the heat flux at the CMB. The seismic observations of thermochemical heterogeneities and partial melting in the D"-region provide additional information to anchor the CMB temperature (Herzberg et al., 2013; Rost et al., 2005; Wen and Helmberger, 1998). It has been argued that the thermochemical piles present in this region could be interpreted as patches of post-bridgmanite (PBg) embedded in bridgmanite (Bg), which would require a double crossing of the Bg-PBg phase transition (Hernlund et al., 2005). Using the P-T Clapeyron slope of the polymorphic transition, this situation is possible if a sharp temperature change occurs when approaching the CMB, for a CMB temperature higher than 4000 K. This method based on the phase diagram of an *unrealistically* pure $MgSiO_3$ end-member has been subsequently challenged by experiments performed on the geophysically relevant Al-bearing $(Mg,Fe)SiO_3$ Bg (Andrault et al., 2010; Catalli et al., 2009). Still, the argument for a double crossing may stand for a partial and progressive transition in Bg (Hernlund, 2010).

The CMB temperature can also be constrained using the melting curve of the silicate mantle. The non-ubiquitous character of the seismic features in the D"-layer forces the CMB temperature to be lower than the mantle solidus. Otherwise, there would be a continuous melting line below which the mantle would be partially molten, due to higher temperatures in the thermal boundary layer when approaching the CMB. The solidus of chondritic-type material plots at 4150 (+/-150) K at a CMB pressure of 135 GPa (Andrault et al., 2011), very close to that of the peridotitic-type mantle (Fiquet et al., 2010). This solidus temperature should actually remain valid for any reasonable mineralogical system composed of Bg, $CaSiO_3$-perovskite and (Mg,Fe)O-ferropericlase, because of the pseudo-eutectic behavior. In contrast, the solidus temperature could be lowered in the presence of a high FeO-content (Mao et al., 2005), high volatile contents (Nomura et al., 2014) or when the excess mantle ferropericlase is replaced by an excess SiO_2, *e.g.*, for a basaltic composition (Andrault et al., 2014). Water can have a dramatic effect, lowering the solidus temperature to ~3570 K, but it is unlikely that

the lower mantle contains a very high water content (Bolfan-Casanova et al., 2003). In contrast, the descent of slabs toward the CMB is clearly imaged by seismic tomography (Grand et al., 1997), and slabs may very well reach the CMB. The solidus temperature of a mid-ocean ridge basalt at the CMB was reported to be 3800 (+/-150) K (Andrault et al., 2014), which suggests that a CMB temperature of 4000 (+/-200) K would produce non-ubiquitous regions of partial melt, in agreement with seismic observations (Fig. 2a).

3.3 The core

The melting curve of pure iron was a long-running source of controversy until recent experimental measurements using laser-heated diamond anvil cells fell in perfect agreement with shock-wave data and ab-initio calculations (Anzellini et al., 2013) (Fig. 2b). The originality of this experiment is fast heating, to prevent the sample pollution from C diffusing out of the diamond anvils, together with the *in situ* detection of sample melting using X-ray diffraction. It suggests a melting temperature of pure Fe at the inner core boundary (ICB) of 6230 (+/- 500) K. The light elements present in the outer core at a level of 10 wt% should lower this melting point. The melting-temperature depletion induced by the presence of S, O and Si are 100, 50 or 30 K/wt%, respectively. Unfortunately, the nature and combination of light elements in the outer core remain subject to debate. A reasonable composition could be 2.5, 5.0 and 5.0 wt% of S, O and Si, respectively, in agreement with the geochemical constraints (Dreibus and Palme, 1996), the density jump at the ICB (Alfè et al., 2002) and the seismic profiles (Vp, ρ) in the outer core (Morard et al., 2013). For this Fe-alloy composition, the melting-temperature depletion can be estimated to 650 (+/- 100) K. This yields an ICB temperature of 5580 (+/- 600) K.

When this anchor point is extrapolated to the CMB using the equation of state of Fe, it yields a CMB temperature of 4100 K, if we assume a constant Grüneisen parameter of 1.51 (Vocadlo et al., 2003). The relative changes in the cocktail of light elements would not drastically change this extrapolated CMB temperature. We note that regardless of the thermal model considered for the core, the heat flux at the CMB remains moderate. Thermal boundary layer(s) with a large temperature jump are unlikely to develop inside the liquid outer core. Therefore, the CMB temperature is a good proxy to discuss the core temperatures, using a relevant adiabatic profile. Based on the melting diagram of the Fe-alloy, the inner core should disappear for CMB temperatures above ~4250 K. This temperature is only a couple hundred degrees above the current CMB temperature and is also just above the mantle solidus of ~4150 K. This indicates that the onset of the inner core crystallization is expected to happen before the lowermost mantle completely solidified.

4. Secular cooling of the deep Earth? Major unresolved paradoxes

These different lines of reasoning converge to the remarkable conclusion that today the CMB temperature is precisely at, or just below, the solidus of the silicate mantle, at 4100 K (+/- 200) K. If the Earth has been cooling for the last ~4.5 Gy, the early core would need to be significantly hotter in the past and, hence, overlaid by molten mantle, a primordial basal magma ocean (BMO) giving birth later to the D"-layer (Labrosse et al., 2007). In this article, we challenge this classic view of Earth's secular cooling based on three major paradoxes:

(i) Since when (and for how much additional time) the CMB temperature has (and will) remain *precisely* just below the solidus of the silicate mantle? It would be very unusual if this peculiar situation were a pure coincidence, since this temperature corresponds to a major change in the mantle state through a first-order phase transformation (the onset of melting at the solidus).

(ii) Producing the geodynamo by a combination of thermal buoyancy and compositional convection (Buffett, 2000) requires a heat flux through the CMB of possibly up to ~10-15 terawatts (TW), depending on the controversial values of electrical and thermal conductivities of the outer core (Pozzo et al., 2012; Zhang et al., 2015). Three ingredients have been advanced to explain the persistence of a significant CMB heat flux from the oldest (4.2 Gy ago) evidences of paleo-magnetic field (Tarduno et al., 2015) to the present day: (a) The first is a tremendous initial core temperature of 5000-7000 K (Davies et al., 2015; Labrosse, 2015; Nakagawa and Tackley, 2010), well above the mantle solidus and even above the liquidus. Such high temperatures would delay the crystallization of the inner core, possibly to a period as late as 0.7 Gy ago (Labrosse, 2015), even if such a late start is still controversial (Biggin et al., 2015). (b) The second ingredient is a high concentration of radiogenic K in the core. Experimental determination of the K partitioning between metal and silicate suggests a maximum of 250 ppm K in the core (Bouhifd et al., 2007), while values below 50 ppm K appear more likely (Corgne et al., 2007; Watanabe et al., 2014). However, models of core cooling with values as high as 400–800 ppm K are not capable of sustaining the geodynamo until the present (Nakagawa and Tackley, 2010). (c) It was suggested that layered structures in the lowermost mantle (Nakagawa and Tackley, 2014) or at the top of the core (Buffett, 2014) may help to retain heat within the core, but the density contrast needs to be large to maintain a gravitationally stable liquid layer in the highly turbulent flows expected in a very hot Earth. Such a global density stratification in the mantle or in the core has not been observed seismically.

(iii) The large initial temperature required for the primordial core implies large fractions of melt in the lowermost mantle. However, it seems very difficult to maintain a basal magma ocean (BMO) at a temperature significantly above the mantle solidus (or, more precisely, above the viscous transition in the mantle, which correspond to ~40% of partial melting (Abe, 1997). This issue is detailed below) for a long period of time (see (Monteux et al., 2016)). (a) The first reason for this is that the silicate melt viscosity is orders of magnitude lower than that of the solid mantle. To show its

effect, let's assume a temperature jump of 1000 K in a super-adiabatic thermal boundary layer lying above the CMB. For a silicate melt, the boundary layer would be thinner than one meter (Solomatov, 2015), which would drive the heat flux to more than 10^6 TW. This implies a negligible temperature jump at the CMB when the silicate is liquid above the CMB. A detailed calculation of the cooling of a hot primitive core with or without a molten layer above the CMB suggests core cooling 10^6 times faster in the presence of a BMO (Monteux et al., 2011). (b) Another argument is based on the fact that the adiabatic profiles of solid, liquid and partially molten chondritic-type mantle present P-T slopes less steep than the mantle solidus (Andrault et al., 2011; Thomas and Asimow, 2013). This implies that the degree of mantle partial melting should increase with elevation from the CMB, not the contrary. For this reason, having a CMB temperature significantly above the mantle solidus would yield major mantle instabilities. If vertical chemical segregation would eventually produce a BMO with a composition different than the average mantle, the situation would not be drastically different. The temperature profile in the BMO would follow a quasi-adiabatic profile from the hot CMB to the interface between the BMO and the overlaying solid mantle. Then, all arguments raised above remain valid, but with a dominant interface for heat exchange being located between the BMO and the solid mantle, instead of exclusively at the CMB. (c) A last argument is that the hot melt could be unstable in the BMO because it is buoyant. It would travel through the mantle towards the Earth's surface. Unfortunately, this issue remains controversial (Andrault et al., 2012; Nomura et al., 2011).

5. A quasi-constant CMB temperature over geological time

The most likely thermal state after the mantle has achieved a ~stable character is that the BMO became significantly viscous, thus below the typical temperature threshold corresponding to 60% of crystallization. This happens at a CMB temperature of ~4400 K for a chondritic-type mantle (Andrault et al., 2011). We note that a peridotitic mantle would become viscous at a slightly higher temperature (Fiquet et al., 2010), however, this composition is much less relevant to the primitive mantle at the CMB. As discussed above, this final temperature could be achieved in less than 10^8 years and it is weakly dependent on the initial CMB temperature (Lebrun et al., 2013; Sleep et al., 2014; Solomatov, 2015). This gives rise to a new paradox: while the CMB temperature reached ~4400 K early in the Earth's history, it is only a few hundred degrees below today, at a temperature of ~4100 K. We note that the uncertainty on the temperature difference of ~300 K is independent of the uncertainty on the experimental determination of the solidus temperature. Indeed, the early and present-day CMB temperatures (slightly above, and just below, respectively) are determined relative to a same reference that is the solidus of the average mantle at the CMB. The uncertainty on the ~300 K secular cooling of the CMB is estimated to ± 100 K.

Such a stable CMB temperature is compatible with geological constraints on the time evolution of the mantle potential temperature (MPT, i.e. the extrapolation to the planetary surface of the mantle's adiabatic temperature profile). For example, petrological analyses of Archean and Proterozoic basalts (between 1.5 and 3.5 Gy old) preserved at the Earth's surface show primary magma compositions compatible with an MPT only ~200 K greater than today (Herzberg et al., 2010). A similar temperature change is reported between Archean tonalite-trondhjemite-granodiorite associations of 4.0 to 2.5 Gy old (Martin and Moyen, 2002). We note that the CMB temperature and the MPT are not formally linked to each other, due to an adjustable temperature jump in the thermal boundary layer above the CMB. Still, they both refer to the thermal state of the deep Earth.

Because the CMB temperature is intimately linked to the core thermal state, a steady CMB temperature over billions of years excludes core cooling as a major ingredient for driving the geodynamo during this period. There are two alternative sources that can induce the turbulent fluid motion in the outer core needed to produce the geomagnetic field: (i) Chemical buoyancy occurs when light elements (mainly O (Alfè et al., 2002)) are released at the ICB due to inner core growth. This effect becomes significant when the temperature drops below ~4250 K, thus at only ~250 K above the present-day CMB temperature (Fig. 2b). Previous work dedicated to the analysis of the relative effects of compositional and thermal convection suggests that the same magnetic field can be generated with approximately half the heat throughput needed if the geodynamo was purely thermally driven (Gubbins et al., 2004). Still, none of the recent studies suggest that chemical buoyancy could drive alone the geomagnetic field for billions of years (Davies et al., 2015; Labrosse, 2015). Alternatively, (ii) mechanical forcing induced by precession and tidal distortions of the CMB (Dwyer et al., 2011; Le Bars et al., 2015; Tilgner, 2005) could have been a major ingredient to maintain the geomagnetic field, since the formation of the Moon. It could still operate today.

6. Precession and tides, an alternative mechanism to drive the geodynamo

Precession and tidal distortions of a planet's CMB induced by gravitational interactions with a companion (e.g. Earth and Moon) are both capable of generating core turbulence and of sustaining a dynamo with critical magnetic Reynolds numbers comparable to thermal and compositional dynamos (Cebron and Hollerbach, 2014; Tilgner, 2005). Indeed, planetary cores, as any rotating fluid, permit eigenmodes of oscillation called "inertial modes", whose restoring force is the Coriolis force. Precession and tides, seen from the mantle frame of reference as small periodic perturbations of the rotating fluid core, are capable of resonantly exciting those inertial modes, leading to fluid instabilities, turbulence and dynamo action. More specifically, two types of instabilities have been described in the literature, the same generic mechanisms working both for precession and tidal excitations (see details in (Le Bars et al., 2015) and references therein): (1) the direct resonance of

one given inertial mode, whose non-linear interactions produce a localized geostrophic shear layer, which can then destabilize and lead to turbulence (Malkus, 1968; Sauret et al., 2014); (2) the triadic resonance of two inertial modes with the harmonic forcing (Kerswell, 1993, 2002), which can either lead to sustained turbulence or to cycles of growth, saturation and collapse (Le Bars et al., 2010). In either case, it is important to recognize that a resonance is involved: even if the excitation amplitude is small, the resulting flows may be intense, draining their energy from the mechanism sustaining the excited waves, i.e. from the spin-orbit rotational energy of the considered system. Such mechanisms provide an appealing alternative explanation for planetary dynamos when the classical convective model does not apply. For instance, they have been proposed to explain the brief dynamos of the Moon and Mars (Stevenson, 2003), the size of these planets being insufficient to sustain long-lived thermally-driven dynamos. The disappearance of Mars' orbiting companion after it collided into the young planet (Arkani-Hamed, 2009) and the recession of the Moon (Dwyer et al., 2011) accompanied by a decrease in the precession intensity, could explain the end of their magnetic histories.

The question then remains to determine (1) whether or not mechanically forced instabilities are present in the Earth's core, and (2) whether or not the generated flows are sufficiently powerful to explain the geomagnetic field. Regarding the first point, the recent literature indeed shows that the present Earth, in the absence of a convectively imposed magnetic field (as would be the case in our non-conventional model), is subject to both tidal and precession instabilities generating turbulence (see e.g. (Cebron et al., 2012)). The second point has been the subject of a long debate between the seminal work of (Malkus, 1968; Malkus, 1963) and the subsequent studies of Rochester et al. (1975) and Loper (1975). This debate was resolved by (Kerswell, 1996): even if the laminar flows considered by (Rochester et al., 1975) and (Loper, 1975) are insufficient to sustain a dynamo, the expected turbulent states in the Earth's core are largely sufficient, and the huge amount of energy stored in the Earth-Moon-Sun system (spin and orbit) provides very large source of energy to sustain the magnetic field over geological time (see e.g. (Le Bars et al., 2015)).

7. The energy budget to sustain the thermal steady state of the deep Earth

7.1 The core budget

Additional arguments to support this proposal are provided by considering the energy budget of the Earth's rotational dynamics as a whole. Models supported by precise measurements coming from lunar laser ranging indicate that 3.7 TW is continuously injected from the Earth-Moon-Sun orbital system into the Earth system (Munk and Wunsch, 1998; Wunsch and Ferrari, 2004). Models also indicate that 0.2 TW is dissipated into the Earth’s atmosphere and its mantle; direct satellite estimates show that 1 TW is lost to the deep ocean; and the most accurate models indicate additional tidal

dissipation in shallow seas of up to 2 TW (Ferrari, 2015). Hence, 0.5 to 1 TW of the dissipated rotational power is still missing in the current energy budget: it may very well be continuously injected into the outer core, where it can fulfill the energy thirst of the geodynamo, estimated to range between 0.1 to 2 TW (Buffett, 2002; Christensen and Tilgner, 2004). The situation was probably even more favorable in the past, when the Moon was closer to the Earth and when the Earth was rotating faster. Indeed, tidal distortion was previously larger and dissipation measured by the Ekman number was smaller, both ingredients being favorable to instability and turbulence (e.g. (Cebron et al., 2012)). One can thus imagine that throughout the history of the Earth-Moon system, turbulent flows and dynamos have been excited by mechanical forcing, the energy dissipated by both ohmic and viscous dissipations participating into the Moon's recession and deceleration (e.g. (Le Bars et al., 2010)).

In addition to the 0.5 to 1 TW rotational power injected into the core for dynamo action, part of which is ultimately transformed into heat by viscous and Joule dissipation, three sources could significantly contribute to the heat budget: (i) Radioactive disintegration of potassium (^{40}K) could provide between 0.2 to 1.4 TW today (Bouhifd et al., 2007; Buffett, 2002; Corgne et al., 2007; Watanabe et al., 2014), (ii) the latent heat of inner core crystallization contributes 0.3 TW, assuming that its crystallization occurs over a period of ~4.3 Gy. (iii) Finally, we note that despite a global steady state, the core temperature may have decreased from ~4400 K originally to ~4100 K today (Fig. 3). Core cooling by ~300 K over 4.3 Gy would provide an average CMB heat flux of ~2 TW. Adding all contributions, the average heat flux coming out of the core could range between 3.0 and 4.7 TW.

On the other hand, the low range of values for the thermal conductivity of the outer core yields a heat flow along the outer-core adiabat between 1.7 to 3.6 TW (Buffett, 2002). For higher values of the conductivity, as suggested recently (Pozzo et al., 2012; Zhang et al., 2015), the adiabatic heat flow would be more than 10 TW (e.g. (Labrosse, 2015)). This range of values appears significantly higher than the 3.0 to 4.7 TW estimated using our model. We note, however, that the temperature profile in the outer core could very well be slightly sub-adiabatic. It would actually facilitate the vertical thermochemical stratification of the outer-core (Helffrich and Kaneshima, 2013). Dynamos excited by mechanical forcing do not require a super adiabatic temperature in the Earth's outer core: it has already been demonstrated that tidal and precession instabilities exist in a stratified environment, theoretically (Cebron et al., 2012), numerically (Cebron et al., 2010) and experimentally in a cylindrical geometry (Guimbard et al., 2010). Instability involves resonances of gravito-inertial waves rather than inertial waves, the main effect being to decrease the excited vertical wavelengths, with negligible or even positive effects on the instability threshold and growth. The same conclusion has been reached concerning other types of unstable flow, for instance Taylor-Couette flows (Le Bars and Le Gal, 2007): contrary to intuition, stratification is capable of increasing flow instability, and

turbulence may develop while maintaining an overall global stratification. In addition to tides and precession, a dynamo driven by the solidification of the inner core could also lead to an overall subadiabiatic core, as studied for the case of Mercury (Manglik et al., 2010).

7.2 The thermal boundary layer in the lowermost mantle

The way the CMB heat flux, estimated above in the range of 3.0 to 4.7 TW from the core energy budget, is accommodated in the lowermost mantle depends on 3 major parameters: (i) the thickness of the thermal boundary layer (e_{TBL}) where conduction is the dominant mechanism of heat transfer. e_{TBL} is generally assumed to be the thickness of the D"-layer, thus 100 to 300 km, as reported by seismological studies (e.g. (Lay et al., 2004)). However, we note that the seismic anomalies used to define e_{TBL} are likely to be preferentially concentrated in the hottest (thus deepest) part of the TBL where the temperature approaches the mantle solidus. At larger distances from the CMB, the temperature profile could still be steeper than in the adiabatic profile (as expected within a TBL), which would however not produce detectable seismic anomalies because of the relatively lower temperatures. (ii) The thermal conductivity *k* of the lowermost mantle, which remains subject to controversial reports. A recent study based on *ab initio* calculations proposed *k*= 3.5 W/m/K for bridgmanite-$MgSiO_3$ (Tang et al., 2014), a value that could be even lowered, by up to 50%, if accounting for the presence of Fe and Al in the Bg-lattice (Manthilake et al., 2011). On the other hand, values up to 16 W/m/K have been proposed for $MgSiO_3$ Bg and post-Bg, with a relatively higher (but anisotropic) *k* value for post-Bg (Ohta et al., 2012). Also, intermediate values of 7-8 W/m/K were recently proposed, for the $MgSiO_3$ end-member again (Stackhouse et al., 2015). (iii) The difference (ΔT_{TBL}) between the CMB temperature (4100 +/- 200 K) and the mantle temperature a few hundred kilometers above the CMB as extrapolated from the adiabatic profile (2600 +/- 200 K). The temperature jump in the TBL could be ~1500 K (Fig. 2).

Using reasonable values of e_{TBL}=200 km, *k*=5 W/m/K, and ΔT_{TBL}=1500 K, we calculate a heat flux at the CMB of ~3.6 TW. This value falls well within the validity limit of our model that is 3 to 4.7 TW. We acknowledge that lower *k* values, or a thicker TLB, would induce a lower CMB heat flux. Considering all possible values of e_{TBL} from 100 to 300 km and *k* from 2 to 8 W/m/K results in plausible CMB heat fluxes ranging from 1.0 to 11.5 TW. Unfortunately, this broad range of uncertainties does not provide additional constraints to our model. We note that it has been suggested that the possible presence of a dense viscous layer above the CMB could help reducing the CMB heat flux (Nakagawa and Tackley, 2014).

On the other hand, based on the heat carried by plumes ascending from the base of the mantle to the Earth's surface, the core heat loss has been estimated to be ~2.3 TW, or perhaps up to 3.5 TW if plumes loose significant amounts of heat during their ascent through the mantle (Davies, 2007). In

401 such thermal budget, it is difficult to take into account the possible deep mantle complexities such as
402 the cooling effect of plate tectonics, the insulating effect of a dense basal layer or also the importance
403 of heat sources available in an enriched deep mantle, because the amplitude of these effects remain
404 highly uncertain. One could argue that our estimated value of the CMB heat flux is much lower than
405 that calculated in recent geodynamic models (e.g. (Nakagawa and Tackley, 2014)). However, such
406 models generally assume a fully viscous mantle, even for an initial CMB temperature of 6000 K that
407 is well above the mantle solidus and the viscous limit of 40% of partial melt. As acknowledged in
408 (Nakagawa and Tackley, 2014), this artificially maintains a hot core for a long period of time,
409 associated with a substantial CMB flux. In a recent study, it was instead shown that an extremely
410 large CMB heat flux prevailed early in the Earth's history, until the viscous transition is reached in
411 the lowermost mantle (Monteux et al., 2016). It yields a CMB temperature of ~4400 K in less than
412 ~1 My after the MFI.
413
414 **8. Implications for geodynamics and major geological events**
415 In addition to generating the Earth's dynamo, turbulent motions excited by astronomical forcing
416 can induce cycles of growth, saturation and abrupt relaxation of the hydrodynamic instabilities
417 (Kerswell, 1993; Sauret et al., 2014). The collapses could induce an abrupt release of energy,
418 potentially up to 10^9 TW (Kerswell, 1996) over short periods of time, in addition to the resonances
419 in the Earth-Moon-Sun spin-orbit system (Greff-Lefftz and Legros, 1999). The pulse duration could
420 vary from a couple periods of rotation (a couple of days) to several hundred years. This corresponds
421 to a broad range of thermal energy release, which could induce core heating by a few to a few hundred
422 of degrees, depending on the integrated pulse amplitude. We note that the 0.5 to 1 TW currently
423 dissipated into the Earth's outer core from the Earth-Moon-Sun orbital system cannot heat the core
424 more than a couple hundred degrees. However, much larger heat pulses could have happened in the
425 past when the Moon was closer to the Earth and when the Earth was rotating faster (Fig. 3).
426 Such fluctuations of the CMB temperature could have two major consequences. (a) Following
427 the adiabatic temperature profile of the Fe-alloy from the CMB to the ICB, they should induce
428 fluctuations in the size of the inner core (Fig. 2b): The abrupt release of hydrodynamic instabilities
429 could reduce the size of the inner core and restore its capability to produce the geodynamo by
430 chemical buoyancy, when the CMB temperature would eventually decrease again by cooling due to
431 weaker dissipation by mechanical forcing. The possibility that an old inner core has undergone several
432 changes in its size, with a rapid decrease and slow increase of its radius could be important for
433 building the inner core anisotropy (Poupinet et al., 1983) as well as a mushy layer at the top of the
434 inner core (Loper and Fearn, 1983). Indeed, both geophysical interpretation are closely related to the
435 mechanism of inner core crystallization (b) On the other hand, partial melting in the lowermost mantle

436 could act as an efficient agent for transferring the excess heat of the core to the overlying mantle:
437 Increasing the temperature above the mantle solidus at the CMB would result in an increase in the
438 degree of partial melting in the lowermost mantle, which in turn would induce a larger CMB heat
439 flux. This mechanism could damp the fluctuations in heat production in the turbulent outer core
440 yielding a ~fixed CMB temperature, precisely at, or just below, the mantle solidus. This thermal state
441 corresponds well to the present-day view of the D”-layer, where piles of partially molten silicate
442 material (the ultra-low velocity zones) interact with mantle convection. Adding heat to the current
443 lowermost mantle would certainly enhance partial melting and the thermal instabilities (inset in Fig.
444 3). As a result, one should expect an increase of the volcanic activity at the Earth's surface shortly
445 after the influx of heat at the CMB (Greff-Lefftz and Legros, 1999). If the brutal energy influx is
446 important, this could explain dramatic eruptions such as the Deccan Trapps (Courtillot and Fluteau,
447 2010), as well as the periodic growth of continents at the Earth's surface (Arndt and Davaille, 2013;
448 Martin et al., 2014).
449 Finally, because the Moon appears to be a necessary ingredient to sustain the magnetic field, and
450 because a magnetic field is needed to shield the Earth’s atmosphere from erosion by solar wind (*e.g.*
451 (Dehant et al., 2007)), the habitability of Earth-like planet may be subordinated to the existence of a
452 large-satellite. While more than 1000 exoplanets have already been observed, the detection of an
453 accompanying exo-moon is rare (Bennett et al., 2014). Hence, our model could have major
454 implications in future planetary missions as exoplanets with orbiting moons would more likely host
455 extraterrestrial life.
456

References:

Abe, Y., 1997. Thermal and chemical evolution of the terrestrial magma ocean. Phys. Earth Planet. Inter. 100, 27-39.

Alfè, D., Gillan, M.J., Price, G.D., 2002. Composition and temperature of the Earth's core constrained by combining ab initio and seismic data. Earth Planet. Sci. Lett. 195, 91-98.

Andrault, D., Bolfan-Casanova, N., Lo Nigro, G., Bouhifd, M.A., Garbarino, G., Mezouar, M., 2011. Melting curve of the deep mantle applied to properties of early magma ocean and actual core-mantle boundary. Earth Planet. Sci. Lett. 304, 251-259.

Andrault, D., Munoz, M., Bolfan-Casanova, N., Guignot, N., Perrillat, J.P., Aquilanti, G., Pascarelli, S., 2010. Experimental evidence for perovskite and post-perovskite coexistence throughout the whole D" region. Earth Planet. Sci. Lett. 293, 90-96.

Andrault, D., Pesce, G., Bouhifd, M.A., Bolfan-Casanova, N., Henot, J.M., Mezouar, M., 2014. Melting of subducted basalt at the core-mantle boundary. Science 344, 892-895.

Andrault, D., Petitgirard, S., Lo Nigro, G., Devidal, J.L., Veronesi, G., Garbarino, G., Mezouar, M., 2012. Solid-liquid iron partitioning in Earth's deep mantle. Nature 487, 354-357.

Anzellini, S., Dewaele, A., Mezouar, M., Loubeyre, P., Morard, G., 2013. Melting of Iron at Earth's Inner Core Boundary Based on Fast X-ray Diffraction. Science 340, 464-466.

Arkani-Hamed, J., 2009. Did tidal deformation power the core dynamo of Mars? Icarus 201, 31-43.

Arndt, N., Davaille, A., 2013. Episodic Earth evolution. Tectonophysics 609, 661-674.

Bennett, D.P., Batista, V., Bond, I.A., Bennett, C.S., Suzuki, D., Beaulieu, J.P., Udalski, A., Donatowicz, J., Bozza, V., Abe, F., Botzler, C.S., Freeman, M., Fukunaga, D., Fukui, A., Itow, Y., Koshimoto, N., Ling, C.H., Masuda, K., Matsubara, Y., Muraki, Y., Namba, S., Ohnishi, K., Rattenbury, N.J., Saito, T., Sullivan, D.J., Sumi, T., Sweatman, W.L., Tristram, P.J., Tsurumi, N., Wada, K., Yock, P.C.M., Albrow, M.D., Bachelet, E., Brillant, S., Caldwell, J.A.R., Cassan, A., Cole, A.A., Corrales, E., Coutures, C., Dieters, S., Prester, D.D., Fouque, P., Greenhill, J., Horne, K., Koo, J.R., Kubas, D., Marquette, J.B., Martin, R., Menzies, J.W., Sahu, K.C., Wambsganss, J., Williams, A., Zub, M., Choi, J.Y., DePoy, D.L., Dong, S., Gaudi, B.S., Gould, A., Han, C., Henderson, C.B., McGregor, D., Lee, C.U., Pogge, R.W., Shin, I.G., Yee, J.C., Szymanski, M.K., Skowron, J., Poleski, R., Kozllowski, S., Wyrzykowski, L., Kubiak, M., Pietrukowicz, P., Pietrzynski, G., Soszynski, I., Ulaczyk, K., Tsapras, Y., Street, R.A., Dominik, M., Bramich, D.M., Browne, P., Hundertmark, M., Kains, N., Snodgrass, C., Steele, I.A., Dekany, I., Gonzalez, O.A., Heyrovsky, D., Kandori, R., Kerins, E., Lucas, P.W., Minniti, D., Nagayama, T., Rejkuba, M., Robin, A.C., Saito, R., Collaboration, M.O.A., Collaboration, P., Collaboration, F.U.N., Collaboration, O., RoboNet, C., 2014. MOA-2011-BLG-262Lb: A sub-Earth-mass moon orbiting a gas giant primary or a high velocity planetary system in the galactic bulge. Astrophysical Journal 785.

Biggin, A.J., Piispa, E.J., Pesonen, L.J., Holme, R., Paterson, G.A., Veikkolainen, T., Tauxe, L., 2015. Palaeomagnetic field intensity variations suggest Mesoproterozoic inner-core nucleation. Nature 526, 245-+.

Bolfan-Casanova, N., Keppler, H., Rubie, D.C., 2003. Water partitioning at 660 km depth and evidence for very low water solubility in magnesium silicate perovskite. Geophys. Res. Lett. 30, L017182.

Bouhifd, M.A., Gautron, L., Bolfan-Casanova, N., Malavergne, V., Hammouda, T., Andrault, D., Jephcoat, A.P., 2007. Potassium partitioning into molten iron alloys at high-pressure: Implications for Earth's core. Phys. Earth Planet. Inter. 160, 22-33.

Brown, J.M., Shankland, T.J., 1981. Thermodynamic parameters in the Earth as determined from seismic profiles. Geoph. J . R. astr. Soc. 66, 579-596.

Buffett, B., 2014. Geomagnetic fluctuations reveal stable stratification at the top of the Earth's core. Nature 507, 484-487.

Buffett, B.A., 2000. Earth's core and the geodynamo. Science 288, 2007-2012.

508 Buffett, B.A., 2002. Estimates of heat flow in the deep mantle based on the power requirements for
509 the geodynamo. Geophys. Res. Lett. 29.
510 Bunge, H.P., Ricard, Y., Matas, J., 2001. Non-adiabaticity in mantle convection. Geophys. Res.
511 Lett. 28, 879-882.
512 Catalli, K., Shim, S.H., Prakapenka, V.B., 2009. Thickness and Clapeyron slope of the post-
513 perovskite boundary. Nature 462, 782-785.
514 Cebron, D., Hollerbach, R., 2014. Tidally driven dynamos in a rotating sphere. Astrophys. J., Lett.
515 789.
516 Cebron, D., Le Bars, M., Moutou, C., Le Gal, P., 2012. Elliptical instability in terrestrial planets and
517 moons. Astronomy & Astrophysics 539.
518 Cebron, D., Maubert, P., Le Bars, M., 2010. Tidal instability in a rotating and differentially heated
519 ellipsoidal shell. Geophys. J. Int. 182, 1311-1318.
520 Christensen, U.R., Tilgner, A., 2004. Power requirement of the geodynamo from ohmic losses in
521 numerical and laboratory dynamos. Nature 429, 169-171.
522 Corgne, A., Keshav, S., Fei, Y., McDonough, W.F., 2007. How much potassium is in the Earth's
523 core? New insights from partitioning experiments. Earth Planet. Sci. Lett. 256, 567-576.
524 Courtillot, V., Fluteau, F., 2010. Cretaceous Extinctions: The Volcanic Hypothesis. Science 328,
525 973-974.
526 Davies, C., Pozzo, M., Gubbins, D., Alfe, D., 2015. Constraints from material properties on the
527 dynamics and evolution of Earth's core. Nat. Geosci. 8, 678-+.
528 Davies, G.F., 2007. Mantle regulation of core cooling: A geodynamo without core radioactivity?
529 Phys. Earth Planet. Inter. 160, 215-229.
530 Deguen, R., Olson, P., Cardin, P., 2011. Experiments on turbulent metal-silicate mixing in a magma
531 ocean. Earth Planet. Sci. Lett. 310, 303-313.
532 Dehant, V., Lammer, H., Kulikov, Y.N., Griessmeier, J.M., Breuer, D., Verhoeven, O., Karatekin,
533 O., Van Hoolst, T., Korablev, O., Lognonne, P., 2007. Planetary magnetic dynamo effect on
534 atmospheric protection of early earth and mars. Space Science Reviews 129, 279-300.
535 Dreibus, G., Palme, H., 1996. Cosmochemical constraints on the sulfur content in the Earth's core.
536 Geochim. Cosmochim. Acta 60, 1125-1130.
537 Dwyer, C.A., Stevenson, D.J., Nimmo, F., 2011. A long-lived lunar dynamo driven by continuous
538 mechanical stirring. Nature 479, 212-284.
539 Ferrari, R., 2015. Personal communication.
540 Fiquet, G., Auzende, A.L., Siebert, J., Corgne, A., Bureau, H., Ozawa, H., Garbarino, G., 2010.
541 Melting of Peridotite to 140 Gigapascals. Science 329, 1516-1518.
542 Frost, D.J., Dolejs, D., 2007. Experimental determination of the effect of H2O on the 410-km
543 seismic discontinuity. Earth Planet. Sci. Lett. 256, 182-195.
544 Grand, S.P., Van der Hilst, R.D., Widiyantoro, S., 1997. High resolution global tomography: a
545 snapshot of convection in the Earth. Geological Society of America Today 7, 1-7.
546 Greff-Lefftz, M., Legros, H., 1999. Core rotational dynamics and geological events. Science 286,
547 1707-1709.
548 Gubbins, D., Alfe, D., Masters, G., Price, G.D., Gillan, M., 2004. Gross thermodynamics of two-
549 component core convection. Geophys. J. Int. 157, 1407-1414.
550 Guimbard, D., Le Dizes, S., Le Bars, M., Le Gal, P., Leblanc, S., 2010. Elliptic instability of a
551 stratified fluid in a rotating cylinder. J. Fluid Mech. 660, 240-257.
552 Helffrich, G., Kaneshima, S., 2013. Causes and consequences of outer core stratification. Phys.
553 Earth Planet. Inter. 223, 2-7.
554 Hernlund, J.W., 2010. On the interaction of the geotherm with a post-perovskite phase transition in
555 the deep mantle. Phys. Earth Planet. Inter. 180, 222-234.
556 Hernlund, J.W., Thomas, C., Tackley, P.J., 2005. A doubling of the post-perovskite phase boundary
557 and structure of the Earth's lowermost mantle. Nature 434, 882-886.
558 Herzberg, C., Asimow, P.D., Ionov, D.A., Vidito, C., Jackson, M.G., Geist, D., 2013. Nickel and
559 helium evidence for melt above the core-mantle boundary. Nature 493, 393-U134.

Herzberg, C., Condie, K., Korenaga, J., 2010. Thermal history of the Earth and its petrological expression. Earth Planet. Sci. Lett. 292, 79-88.
Katsura, T., Yoneda, A., Yamazaki, D., Yoshino, T., Ito, E., 2010. Adiabatic temperature profile in the mantle. Phys. Earth Planet. Inter. 183, 212-218.
Ke, Y., Solomatov, V.S., 2009. Coupled core-mantle thermal evolution of early Mars. J. Geophys. Res.: Planets 114.
Kerswell, R.R., 1993. The instability of precessing flow. Geophys. Astrophys. Fluid Dyn. 72, 107-144.
Kerswell, R.R., 1996. Upper bounds on the energy dissipation in turbulent precession. J. Fluid Mech. 321, 335-370.
Kerswell, R.R., 2002. Elliptical instability. Annu. Rev. Fluid Mech. 34, 83-113.
Kleine, T., Munker, C., Mezger, K., Palme, H., 2002. Rapid accretion and early core formation on asteroids and the terrestrial planets from Hf-W chronometry. Nature 418, 952-955.
Labrosse, S., 2015. Thermal evolution of the core with a high thermal conductivity. Phys. Earth Planet. Inter., In press.
Labrosse, S., Hernlund, J.W., Coltice, N., 2007. A crystallizing dense magma ocean at the base of the Earth's mantle. Nature 450, 866-869.
Lay, T., Garnero, E.J., Williams, Q., 2004. Partial melting in a thermo-chemical boundary layer at the base of the mantle. Phys. Earth Planet. Inter. 146, 441-467.
Le Bars, M., Cébron, D., Le Gal, P., 2015. Flows Driven by Libration, Precession, and Tides. Annu. Rev. Fluid Mech. 47, 163-193.
Le Bars, M., Lacaze, L., Le Dizes, S., Le Gal, P., Rieutord, M., 2010. Tidal instability in stellar and planetary binary systems. Phys. Earth Planet. Inter. 178, 48-55.
Le Bars, M., Le Gal, P., 2007. Experimental analysis of the stratorotational instability in a cylindrical couette flow. Phys. Rev. Lett. 99.
Lebrun, T., Massol, H., Chassefiere, E., Davaille, A., Marcq, E., Sarda, P., Leblanc, F., Brandeis, G., 2013. Thermal evolution of an early magma ocean in interaction with the atmosphere. J. Geophys. Res.: Planets 118, 1155-1176.
Loper, D.E., 1975. Torque balance and energy budget for precessional driven dynamo. Phys. Earth Planet. Inter. 11, 43-60.
Loper, D.E., Fearn, D.R., 1983. A seismic model of partially molten inner core. J. Geophys. Res. 88, 1235-1242.
Malkus, W., V, R, 1968. Precession of the Earth as the cause of geomagnetism. Science 160, 259-264.
Malkus, W.V.R., 1963. Precessional torques as cause of geomagnetism. J. Geophys. Res. 68, 2871-&.
Manglik, A., Wicht, J., Christensen, U.R., 2010. A dynamo model with double diffusive convection for Mercury's core. Earth Planet. Sci. Lett. 289, 619-628.
Manthilake, G.M., de Koker, N., Frost, D.J., McCammon, C.A., 2011. Lattice thermal conductivity of lower mantle minerals and heat flux from Earth's core. Proc. Natl. Acad. Sci. U. S. A. 108, 17901-17904.
Mao, W.L., Meng, Y., Shen, G., Prakapenka, V.B., Campbell, A.J., Heinz, D.L., Shu, J., Caracas, R., Cohen, R.E., Fei, Y., Hemley, R.J., Mao, H.K., 2005. Iron-rich silicate in the Earth’s D" layer. Proc. Natl. Acad. Sci. U. S. A. 102, 9751–9753.
Martin, H., Moyen, J.F., 2002. Secular changes in tonalite-trondhjemite-granodiorite composition as markers of the progressive cooling of Earth. Geology 30, 319-322.
Martin, H., Moyen, J.F., Guitreau, M., Blichert-Toft, J., Le Pennec, J.L., 2014. Why Archaean TTG cannot be generated by MORB melting in subduction zones. Lithos 198, 1-13.
Matas, J., Bass, J.D., Ricard, Y., Mattern, E., Bukowinsky, M.S., 2007. On the bulk composition of the lower mantle: predictions and limitations from generalized inversion of radial seismic profiles. Geophys. J. Int. 170, 764-780.

611 Monteux, J., Andrault, D., Samuel, H., 2016. On the cooling of a deep terrestrial magma ocean.
612 Earth Planet. Sci. Lett., submitted.
613 Monteux, J., Jellinek, A.M., Johnson, C.L., 2011. Why might planets and moons have early
614 dynamos? Earth Planet. Sci. Lett. 310, 349-359.
615 Monteux, J., Ricard, Y., Coltice, N., Dubuffet, F., Ulvrova, M., 2009. A model of metal-silicate
616 separation on growing planets. Earth Planet. Sci. Lett. 287, 353-362.
617 Morard, G., Siebert, J., Andrault, D., Guignot, N., Garbarino, G., Guyot, F., Antonangeli, D., 2013.
618 The Earth's core composition from high pressure density measurements of liquid iron alloys. Earth
619 Planet. Sci. Lett. 373, 169-178.
620 Munk, W., Wunsch, C., 1998. Abyssal recipes II: energetics of tidal and wind mixing. Deep-Sea
621 Res.Pt I 45, 1977-2010.
622 Nakagawa, T., Tackley, P.J., 2010. Influence of initial CMB temperature and other parameters on
623 the thermal evolution of Earth's core resulting from thermochemical spherical mantle convection.
624 Geochem., Geophys., Geosyst. 11, Q06001.
625 Nakagawa, T., Tackley, P.J., 2014. Influence of combined primordial layering and recycled MORB
626 on the coupled thermal evolution of Earth's mantle and core. Geochem., Geophys., Geosyst. 15,
627 619-633.
628 Nakajima, M., Stevenson, D.J., 2015. Melting and Mixing States of the Earth's Mantle after the
629 Moon-Forming Impact. Earth Planet. Sci. Lett., in press.
630 Nomura, R., Hirose, K., Uesugi, K., Ohishi, Y., Tsuchiyama, A., Miyake, A., Ueno, Y., 2014. Low
631 Core-Mantle Boundary Temperature Inferred from the Solidus of Pyrolite. Science 343, 522-525.
632 Nomura, R., Ozawa, H., Tateno, S., Hirose, K., Hernlund, J.W., Muto, S., Ishii, H., Hiraoka, N.,
633 2011. Spin crossover and iron-rich silicate melt in the Earth's deep mantle. Nature 473, 199-202.
634 Ohta, K., Yagi, T., Taketoshi, N., Hirose, K., Kornabayashi, T., Baba, T., Ohishi, Y., Hernlund, J.,
635 2012. Lattice thermal conductivity of MgSiO3 perovskite and post-perovskite at the core-mantle
636 boundary. Earth Planet. Sci. Lett. 349, 109-115.
637 Poupinet, G., Pillet, R., Souriau, A., 1983. Possible heterogeneity of the Earth's core deduced from
638 PKIKP travel times. Nature 305, 204-206.
639 Pozzo, M., Davies, C., Gubbins, D., Alfè, D., 2012. Thermal and electrical conductivity of iron at
640 Earth's core conditions. Nature 485, 355-399.
641 Rochester, M.G., Jacobs, J.A., Smylie, D.E., Chong, K.F., 1975. Can precession power
642 geomagnetic dynamo. Geoph. J . R. astr. Soc. 43, 661-678.
643 Rost, S., Garnero, E.J., Williams, Q., Manga, M., 2005. Seismological constraints on a possible
644 plume root at the core-mantle boundary. Nature 435, 666-669.
645 Rubie, D.C., Nimmo, H.J., Melosh, H.J., 2015. Formation of the Earth's core, in: Schubert, G. (Ed.),
646 Treatise on Geophysics, 2 ed. Elsevier, Amsterdam, pp. 43-79.
647 Rudge, J.F., Kleine, T., Bourdon, B., 2010. Broad bounds on Earth's accretion and core formation
648 constrained by geochemical models. Nat. Geosci. 3, 439-443.
649 Samuel, H., 2012. A re-evaluation of metal diapir breakup and equilibration in terrestrial magma
650 oceans. Earth Planet. Sci. Lett. 313, 105-114.
651 Samuel, H., Tackley, P.J., Evonuk, M., 2010. Heat partitioning in terrestrial planets during core
652 formation by negative diapirism. Earth Planet. Sci. Lett. 290, 13-19.
653 Sauret, A., Le Bars, M., Le Gal, P., 2014. Tide-driven shear instability in planetary liquid cores.
654 Geophys. Res. Lett. 41, 6078-6083.
655 Sleep, N.H., Zahnle, K.J., Lupu, R.E., 2014. Terrestrial aftermath of the Moon-forming impact.
656 Philos. Trans. R. Soc., A 372.
657 Solomatov, V.S., 2000. Fluid dynamics of terrestrial magma ocean, in: Canup, R.M., Righter, K.
658 (Eds.), Origin of the Earth and Moon. The University of Arizona Press, Tucson, Arizona, pp. 323-
659 338.
660 Solomatov, V.S., 2015. Magma Oceans and Primordial Mantle Differentiation, in: Schubert, G.
661 (Ed.), Treatise on Geophysics, 2 ed. Elsevier, Amsterdam, pp. 81-104.
662 Stacey, F.D., Davis, P.M., 2008. Physics of the Earth, 4th ed. Cambridge University Press.

Stackhouse, S., Stixrude, L., Karki, B.B., 2015. First-principles calculations of the lattice thermal conductivity of the lower mantle. Earth Planet. Sci. Lett. 427, 11-17.
Stevenson, D.J., 1990. Fluid dynamics of core formation, in: Newsom, H., Jones, J.H. (Eds.), The origin of the Earth. Oxford Press, London, pp. 231-249.
Stevenson, D.J., 2003. Planetary magnetic fields. Earth Planet. Sci. Lett. 208, 1-11.
Tang, X.L., Ntam, M.C., Dong, J.J., Rainey, E.S.G., Kavner, A., 2014. The thermal conductivity of Earth's lower mantle. Geophys. Res. Lett. 41, 2746-2752.
Tarduno, J.A., Cottrell, R.D., Davis, W.J., Nimmo, F., Bono, R.K., 2015. A Hadean to Paleoarchean geodynamo recorded by single zircon crystals. Science 349, 521-524.
Thomas, C.W., Asimow, P.D., 2013. Direct shock compression experiments on premolten forsterite and progress toward a consistent high-pressure equation of state for CaO-MgO-Al2O3-SiO2-FeO liquids. J. Geophys. Res.: Solid Earth 118, 5738-5752.
Tilgner, A., 2005. Precession driven dynamos. Physics of Fluids 17.
Touboul, M., Kleine, T., Bourdon, B., Palme, H., Wieler, R., 2007. Late formation and prolonged differentiation of the Moon inferred from W isotopes in lunar metals. Nature 450, 1206-1209.
Vocadlo, L., Alfe, D., Gillan, M.J., Wood, I.G., Brodholt, J.P., Price, G.D., 2003. Possible thermal and chemical stabilization of body-centred-cubic iron in the Earth's core. Nature 424, 536-539.
Wacheul, J.-B., Le Bars, M., Monteux, J., Aurnou, J.M., 2014. Laboratory experiments on the breakup of liquid metal diapirs. Earth Planet. Sci. Lett. 403, 236-245.
Watanabe, K., Ohtani, E., Kamada, S., Sakamaki, T., Miyahara, M., Ito, Y., 2014. The abundance of potassium in the Earth's core. Phys. Earth Planet. Inter. 237, 65-72.
Wen, L., Helmberger, D.V., 1998. Ultra-Low Velocity Zones Near the Core-Mantle Boundary from Broadband PKP Precursors. Science 279, 1701-1703.
Wunsch, C., Ferrari, R., 2004. Vertical mixing, energy and the general circulation of the oceans. Annu. Rev. Fluid Mech. 36, 281-314.
Zhang, P., Cohen, R.E., Haule, K., 2015. Effects of electron correlations on transport properties of iron at Earth's core conditions. Nature 517, 605-NIL_376.

692 **Figure Captions**

693

694 **Figure 1:** Schematic representation of the Earth's interior evolution from the Moon forming impact
695 (MFI) to the present. Full crystallization of the molten Earth was probably very complex due to
696 suspension, turbulence, nucleation, and percolation processes (Solomatov, 2015). (a) The MFI
697 occurred 50-100 Myr after the formation of the Ca-Al rich inclusions (CAI, the oldest objects in the
698 solar system). It left the Earth mostly molten with a core temperature potentially above 6000 K (Rubie
699 et al., 2015). (b) In the magma ocean, high temperatures and turbulent state should efficiently cool
700 down the deep mantle and the liquid core. This could favor a thermally driven geodynamo.
701 Progressive decrease of the potential temperature below the viscous threshold of 60 % crystallization
702 took within 10^3 to ~10^6 years, essentially depending on the magma ocean viscosity (Monteux et al.,
703 2016). During this time, a thin crust rapidly formed at the Earth's surface. Also, a basal magma ocean
704 could have existed, however, its life time remains controversial (Labrosse et al., 2007; Monteux et
705 al., 2016). Large plumes of hot and/or partially-molten material could have migrated toward the
706 Earth's surface. (c) The final step of mantle solidification could have taken longer, depending on the
707 cooling efficiency at the Earth's surface (Lebrun et al., 2013; Sleep et al., 2014). This period would
708 correspond to progressive decrease of the CMB temperature to the mantle solidus at ~4150 K (Fig.
709 2a), associated with the crystallization and the growth of the inner core (Fig. 2b). This would favor a
710 compositionally driven geodynamo, an ingredient that could still today contribute to sustaining the
711 geodynamo. (d) Later on, the long-term solid-state convection in the mantle, as we currently know it,
712 started. At this period, the CMB temperature could have remained nearly constant for geological
713 times. Because of moderate core cooling and growth of the inner core, a major ingredient to sustain
714 the geodynamo could be mechanical forcing by astronomical forces. In fact, mechanical forcing could
715 have started to induce core motions as soon as the moon was formed. Colors orange to grey
716 (intermediate = yellow) correspond to the mantle encountering a degree of partial melting from 100%
717 to 0% (intermediate=40%), while black and white correspond to liquid (outer) and solid (inner) core,
718 respectively.

719

720 **Figure 2**: Present-day temperature profile in the Earth's (a) mantle and (b) core inferred from
721 several experimental arguments. Green circles correspond to the most likely temperature at the
722 core-mantle boundary. (a) At the CMB pressure of 135 GPa, melting temperatures of 4180, 4150,
723 3800 and 2570 K were reported for peridotite (F-10 (Fiquet et al., 2010)), chondritic-type mantle
724 (A-14 (Andrault et al., 2014)), mid-ocean ridge basalt (A-11 (Andrault et al., 2011)) and wet-
725 pyrolite (N-14 (Nomura et al., 2014)), respectively. Dashed curves stand for adiabatic profiles (M-

07 (Matas et al., 2007), H-05 (Hernlund et al., 2005), K-10 (Katsura et al., 2010), BS-81 (Brown and Shankland, 1981), B-01 (Bunge et al., 2001)). (b) Melting of pure Fe was reported at 4175 and 6230 K for pressure conditions of CMB (135 GPa) and ICB (330 GPa), respectively (A-13 (Anzellini et al., 2013)). A melting temperature depletion of ~650 K can account for the presence of light elements in the core (e.g. (Morard et al., 2013)). The CMB temperature is extrapolated from the ICB based on the adiabatic profile in the outer core.

Figure 3: Schematic evolution of the CMB temperature since the Earth's accretion. In the hypothesis of an initial CMB temperature above 6000 K (Rubie et al., 2015), rapid cooling is expected until the drastic increase in mantle viscosity at the CMB (see text and (Monteux et al., 2016)). It corresponds to a degree of partial melting of ~40% (Abe, 1997), thus a temperature of ~4400 K for a primordial chondritic mantle (Andrault et al., 2011). Then, the complete mantle crystallization could have taken up to more than 1 Gy, as suggested by geodynamic modeling (e.g. (Nakagawa and Tackley, 2010)). After the mantle became significantly viscous, a purely thermally-driven dynamo becomes unlikely due to major slow-down of the CMB heat flux. As a result, the CMB temperature remained close to the mantle solidus, at ~4100 K, until today (see Fig. 2). At a period difficult to define precisely based on our model, the appearance of the inner core (indicating a CMB temperature below ~4250 K) provided buoyancy sources from the release of latent heat and light elements. Still, the sources of energy are insufficient to maintain the geodynamo from the first evidence of geomagnetic field, ~4.2 Gy ago (Tarduno et al., 2015) to present day. This strongly suggests that mechanical forcing induced by a combination of astronomical forces (see (Le Bars et al., 2015)) has been a major ingredient to maintain the geodynamo. Due to the intrinsically time-dependent character of the mechanical forcing, periods of growing instabilities and intense turbulent motions would alternate with cycles of relaxation associated with abrupt releases of large amounts of energy (e.g. (Kerswell, 1993). Abrupt increases of the core temperature, triggering increases in partial mantle melting at the CMB (see inset), could be related to the geological evidence of periods of hot and intense volcanic eruptions (Arndt and Davaille, 2013; Martin et al., 2014).

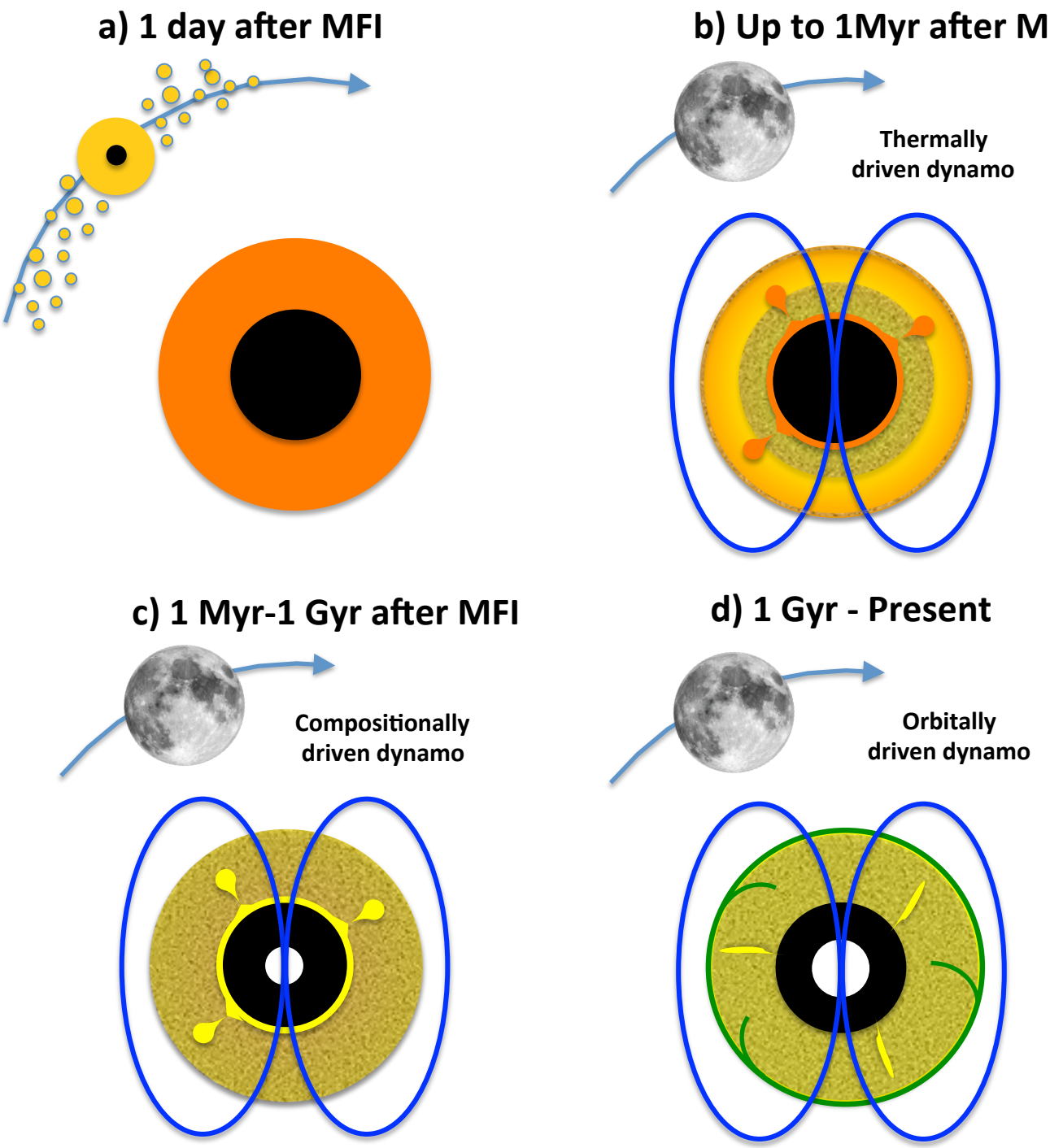
a) 1 day after MFI
b) Up to 1Myr after MFI
Thermally
driven dynamo
c) 1 Myr-1 Gyr after MFI
Compositionally
driven dynamo
d) 1 Gyr - Present
Orbitally
driven dynamo

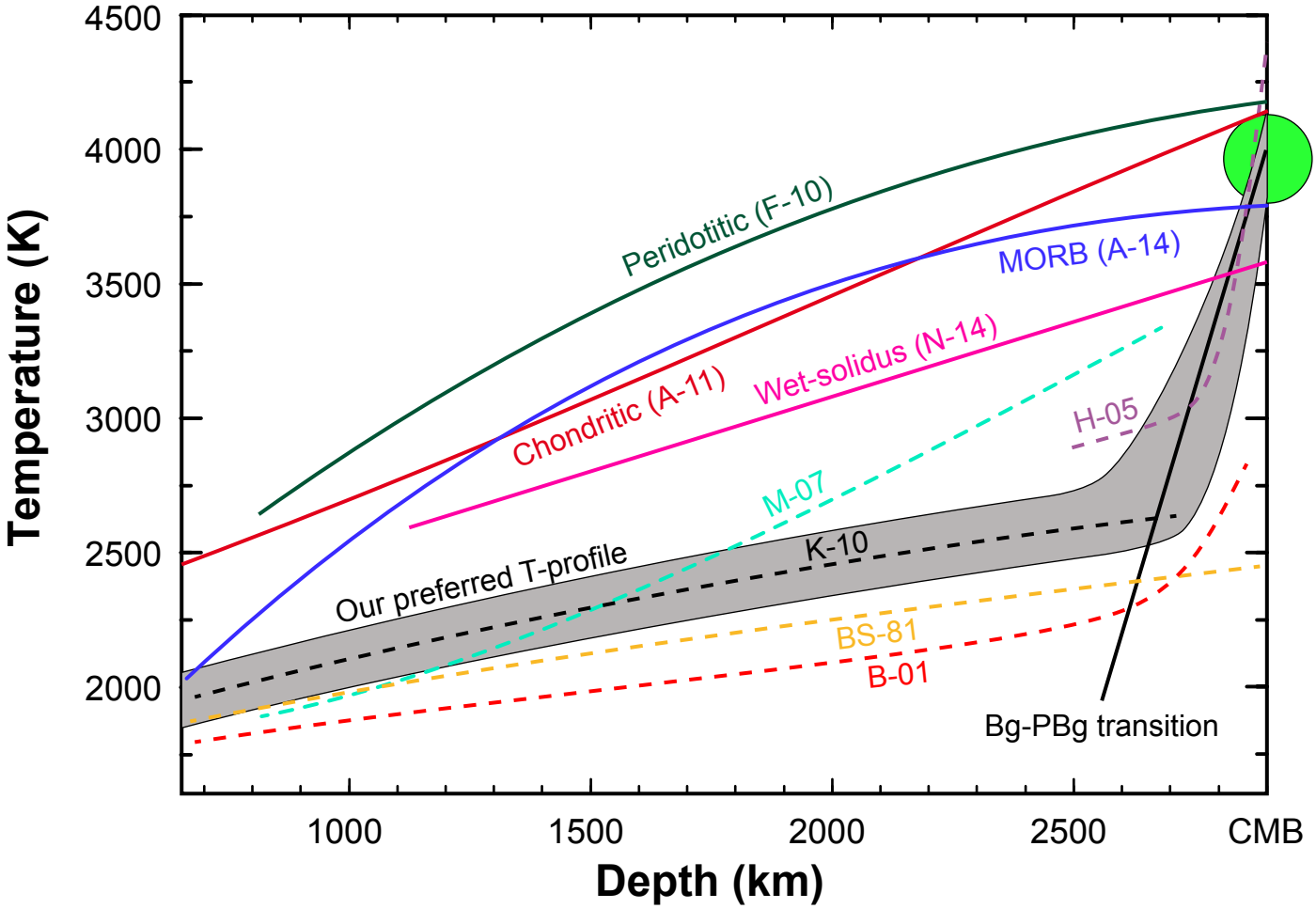
4500
4000
3500
3000
2500
2000
Temperature (K)
1000
1500
2000
2500
CMB
Depth (km)
Peridotitic (F-10)
MORB (A-14)
Chondritic (A-11)
Wet-solidus (N-14)
H-05
M-07
Our preferred T-profile
K-10
BS-81
B-01
Bg-PBg transition

Fig. 2A

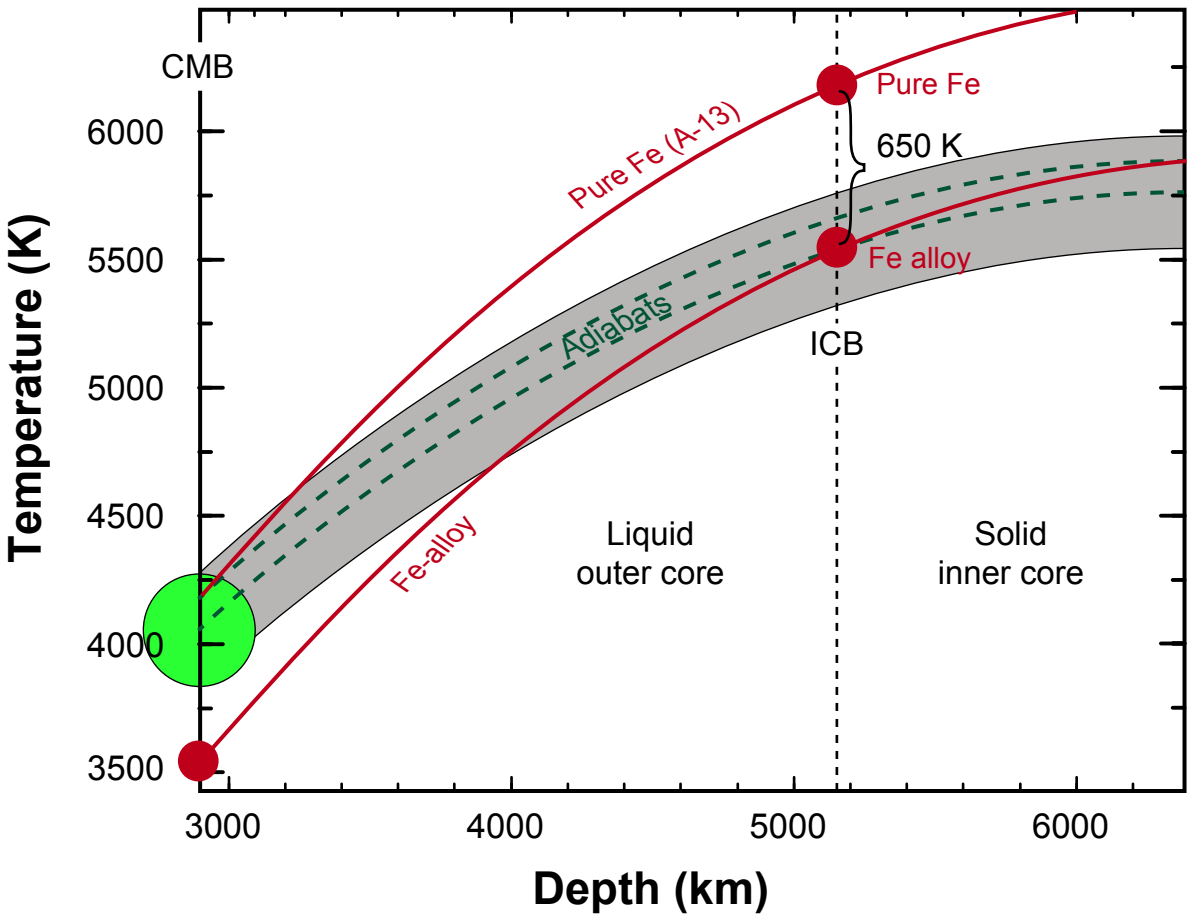
CMB
Pure Fe
650 K
Pure Fe (A-13)
Fe alloy
Adiabats
ICB
Fe-alloy
Liquid
outer core
Solid
inner core
Temperature (K)
6000
5500
5000
4500
4000
3500
3000
4000
5000
6000
Depth (km)

Fig. 2B

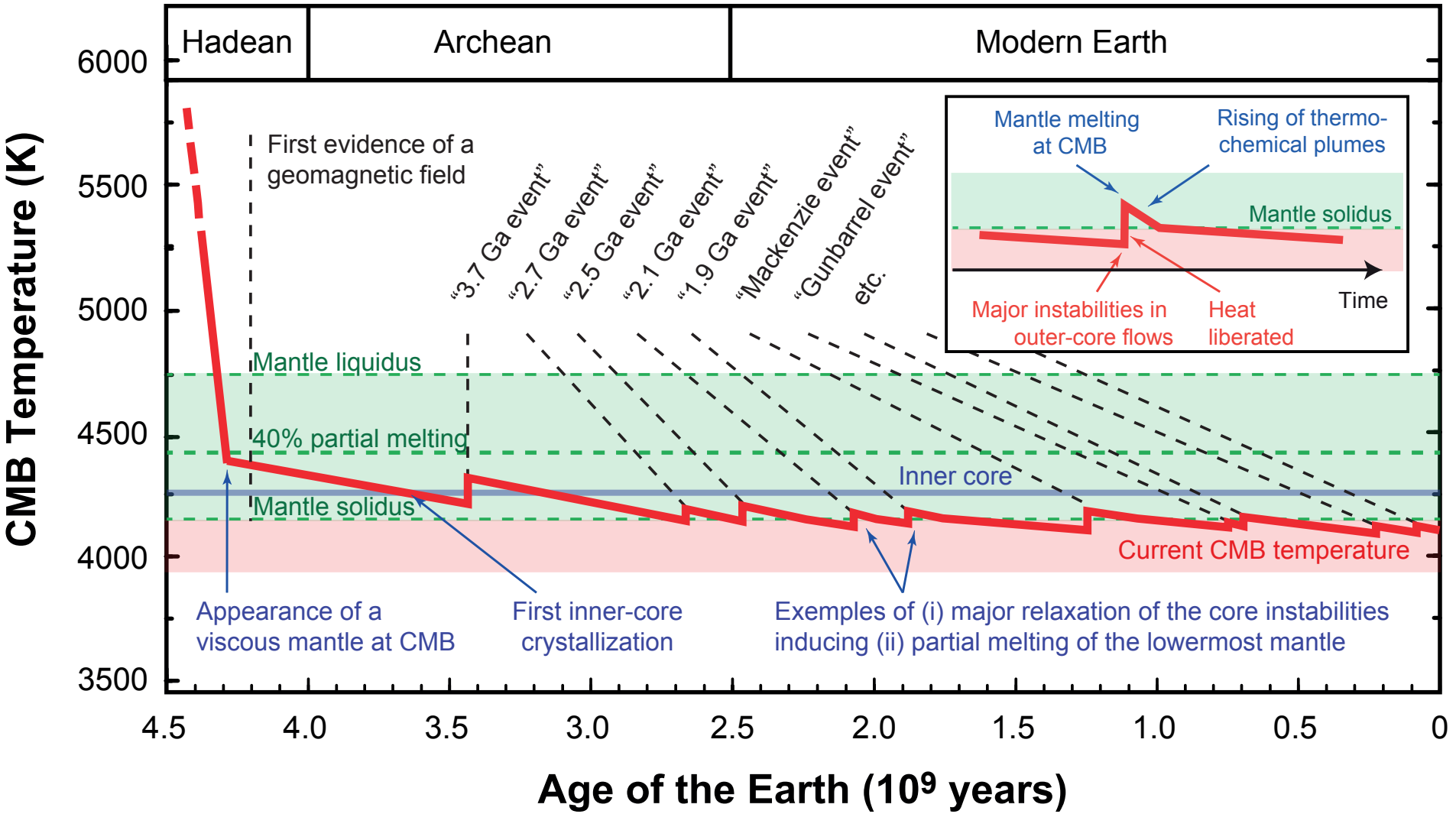
Hadean
Archean
Modern Earth
6000
5500
5000
4500
4000
3500
CMB Temperature (K)
First evidence of a geomagnetic field
"3.7 Ga event"
"2.7 Ga event"
"2.5 Ga event"
"2.1 Ga event"
"1.9 Ga event"
"Mackenzie event"
"Gunbarrel event"
etc.
Mantle liquidus
40% partial melting
Mantle solidus
Inner core
Current CMB temperature
Appearance of a viscous mantle at CMB
First inner-core crystallization
Exemples of (i) major relaxation of the core instabilities inducing (ii) partial melting of the lowermost mantle
Mantle melting at CMB
Rising of thermo-chemical plumes
Mantle solidus
Time
Major instabilities in outer-core flows
Heat liberated
4.5
4.0
3.5
3.0
2.5
2.0
1.5
1.0
0.5
0
Age of the Earth (10⁹ years)